Catalysis Letters, Vol. 118, Nos. 1–2, October 2007 (© 2007)
DOI: 10.1007/s10562-007-9135-4

Liquid phase hydrogenation of maleic anhydride over nickel catalyst supported on ZrO_2–SiO_2 composite aerogels

Chun-guang Gao,[a,b] Yong-xiang Zhao,[a,*] and Dian-sheng Liu[b,*]

[a]*School of Chemistry and Chemical Engineering, Shanxi University, Shanxi, Taiyuan, 030006, P.R. China*
[b]*Institute of Advanced Chemistry, Shanxi University, Shanxi, Taiyuan, 030006, P.R. China*

Received 20 April 2007; accepted 7 May 2007

The promotional effects of ZrO_2 on Ni/ZrO_2–SiO_2 catalysts were investigated by the comparison of Ni/SiO_2 and Ni/ZrO_2–SiO_2 activity in the hydrogenation of maleic anhydride (MA) to γ-butyrolactone (GBL), and by the measurements of X-ray diffraction (XRD), Fourier transform infrared (FT-IR), temperature-programmed reduction (TPR) and ammonia temperature-programmed desorption (NH_3-TPD). The presence of ZrO_2 led to an obvious increase of GBL yield. The promotion effect could be attributed to the possible presence of Zr^{4+} species on the catalyst surface owing to the higher ionicity of the Zr–O bonds, and to the proper interaction of Ni with the ZrO_2-SiO_2 support that is regulated by the presence of ZrO_2.

KEY WORDS: ZrO_2–SiO_2 composite aerogels; γ-butyrolactone; hydrogenation of maleic anhydride; nickel.

1. Introduction

GBL is currently one of the most valuable alternatives to the environmentally harmful chlorinated solvents, which have been widely used in the polymer and paint industries. Hydrogenation of MA is the most direct way to produce GBL and it does not involve the use of hazardous materials. In published works, different catalysts were used in the MA hydrogenation in different ways, such as liquid-phase, gas phase and homogeneous reactions, and the activity performance is dependent on the catalysts active phase, support and promoter.

Uwe Herrmann and Gerhard Emig [1] investigated the liquid phase hydrogenation of MA in a packed bubble column reactor using different copper-based catalysts. A copper-zinc catalyst was found to be active in the formation of 1,4-butanediol (BDO), whereas on zinc-free copper catalysts, mainly succinic anhydride (SA) and GBL were formed. They had also investigated the liquid phase hydrogenation of MA and intermediates in a stirred tank slurry reactor using copper-based and noble metal catalysts [2]. The copper chromites and noble metal catalysts were found to be suitable for the hydrogenation of MA.

R.M. Deshpande et al. [3] investigated the liquid phase hydrogenation of SA to GBL and BDO using ruthenium–cobalt bimetallic catalysts in a semi-batch slurry reactor. It was found that addition of small amounts of ruthenium to cobalt catalyst increased the overall hydrogenation activity of the cobalt catalyst. Ruthenium doping mainly influenced the formation of THF from SA and further hydrogenation of butanediol to propanol. The hydrogenation of GBL to BDO and THF to butanol steps seemed to be independent of ruthenium.

Yoshinori Hara and Kazunari Takahashi [4] prepared a ruthenium catalyst system consisting of Ru salts, trialkylphosphine and *p*-toluene sulfonic acid, which was found very effective for the hydrogenation of SA affording GBL in liquid-phase, and exhibited excellent catalyst performance with exceeding 97% selectivity for GBL and high activity.

Seong Moon Jung et al. [5,6] investigated the promotional effects of Sn on Pd/SiO_2 by the comparison of Pd/SiO_2 and Pd–Sn/SiO_2 activity in the hydrogenation of MA and SA to GBL. As a result, it is proposed that Pd–Sn/SiO_2 catalyst can be an effective one-step catalyst for hydrogenation of MA to GBL. The promotional effect of tin on Pd–Sn/SiO_2 catalyst can be explained by the change of electronic configuration of Pd due to the interaction with Sn. The effective interaction between Pd and Sn in the hydrogenation of MA to GBL is enhanced when the reduction temperature is performed at higher temperature.

Jian Xu et al. [7,8] prepared a Pd/TiO_2 catalyst for the liquid phase hydrogenation of MA. Over Pd/TiO_2 catalyst prepared by sol–gel and super critical fluid of ethanol drying, 93.5% yield to butyric acid and 100% conversion of MA were obtained at 240 °C, 3 MPa.

*To whom correspondence should be addressed.
E-mail: yxzhao@sxu.edu.cn

Heondo Jeong et al. [9] prepared a catalyst composed of palladium, molybdenum and nickel on a silica support of high surface area. This multi-component mixed metal oxide catalyst system in a batch-type reactor is found to be suitable for the hydrogenation of MA selectively to GBL. The hydrogenation of MA using this catalyst is not observed by-products and the selectivity of GBL is very high.

Tongjie Hu et al. [10] prepared Cu–Zn–Ti catalysts by coprecipitation method and applied the catalyst to gas phase hydrogenation of MA to GBL. The Cu–Zn–Ti catalysts with Cu:Zn:Ti ratios of 1:2:1 and 2:2:1.5 showed high catalytic activity in the gas phase hydrogenation of MA to GBL.

In this paper, we report a study on the hydrogenation of maleic anhydride on ZrO_2–SiO_2 composite aerogels and SiO_2 aerogels supported nickel catalysts. The catalysts were characterized by means of XRD, FT-IR, TPR and NH_3-TPD. The aim of this work is to realize an investigation of the effects of the presence of ZrO_2 on supported nickel catalysts. Moreover, the effects of the reaction conditions have also been investigated to taking into account the potential industrial relevance of ''single-step'' hydrogenation of MA to GBL with the Ni/ZrO_2–SiO_2 catalysts.

2. Experiment procedure

2.1. Preparation of catalysts

The synthesis procedure for ZrO_2–SiO_2 composite aerogels and SiO_2 aerogels adapted from that already reported by our group in [11] is described briefly below. A proper amount of zirconyl nitrate dihydrate ($ZrO(NO_3)_2{\cdot}2H_2O$) was dissolved in an ethanol solution, then acetic acid, water and tetraethoxysilicane (TEOS) were added into under constant stirring. The mixture was transferred into an autoclave and heated to the supercritical condition of ethanol (516 K, 6.36 MPa) and kept the conditions for about 0.5 h. Then unclosed the leak valve let the gas leaking slowly from the autoclave, and swept with N_2 before room temperature was reached. The obtained composite aerogels monolith ZrO_2–SiO_2 was crushed into 40–60 mesh. The ZrO_2 content 5 wt. % was selected in this work according to a content selection test (data not shown). The SiO_2aerogels was prepared with the same above process without adding $ZrO(NO_3)_2{\cdot}2H_2O$.

A proper amount of $Ni(NO_3)_2$ was impregnated with the above ZrO_2–SiO_2 and SiO_2 aerogels respectively to obtain Ni/ZrO_2–SiO_2 (catalyst code: 30Ni/ZrO_2–SiO_2) and Ni/SiO_2 (catalyst code: 30Ni/SiO_2) catalysts, and both were calcined at 673 K for 3 h and reduced with hydrogen at 673 K for 3 h. The content of Ni is selected to 30 wt. % according to the previous work of our group [12].

2.2. Characterization of catalysts

Catalysts were characterized with FT-IR (Shimadzu 8400S FT-IR, Japan), XRD (Rigaku D/max 2500, Cu Ka radiation, 50 kV, 60 mA), N_2 adsorption-desorption isotherms (Micromeritics ASAP 2020), TPR, NH_3-TPD and elemental analysis (AtomScan 16).

TPR measurements were carried out from 50 to 700 °C in a conventional lab-made apparatus equipped with a thermal conductivity detector (TCD) under the following conditions: heating rate, 10 °C min^{-1}; flow rate of nitrogen gas containing 10 vol.% of hydrogen, 30 cm^3 min^{-1}; catalyst weight, 30 mg.

NH_3-TPD experiments were also recorded on the above apparatus fitted with a TCD. The samples (0.1 g) were pretreated at 500 °C in a He stream for 2 h in order to remove surface contaminants, and ammonia was absorbed at 50 °C. The heating rate and sweep gas (helium) flow during the measurement of ammonia desorption were 10 °C and 60 cm^3 min^{-1}, respectively.

2.3. Catalytic test

The catalytic hydrogenation of MA (reaction conditions: 453 K, 3.0 MPa, 3 h) in liquid phase was performed on the prepared catalysts within an autoclave (FYX 0.1, Da-Lian No.4 Instrument Plant, China) using 4.9 g MA and 0.1 g catalysts, and THF was charged in the autoclave as solvent. The reactor was heated to the desired temperature while being filled with known amounts of hydrogen based on the set pressure.

The components MA, SA and GBL were analyzed with a gas chromatography (GC-930, Hai-Xin Company, Shanghai China) equipped with a capillary column (SE-52, Lan-zhou Institute of Chemical Physics, China), column temperature was 333 K, and quantitative analysis was performed using a CDP-4A integrator (Wu-Feng Scientific Instruments Ltd. Shanghai, China). Peak areas were converted into concentration using the internal standard normalization.

3. Results and discussion

3.1. Characterization of catalysts

3.1.1. XRD analysis

The features exhibited on the XRD patterns (figure 1.) of the catalysts 30Ni/SiO_2 and 30Ni/ZrO_2–SiO_2 showed Ni and NiO were both existed in the two catalysts and the two catalysts had no obvious difference in crystal structure and particle size. That is, the addition of ZrO_2had no influence on the catalysts crystal structure, and the characteristic peaks of ZrO_2 were not detected meaning that ZrO_2 should be present in amorphous phase. The previous published work of our group [11] has studied the crystal composition of ZrO_2–SiO_2 composite aerogels, and the result suggests when

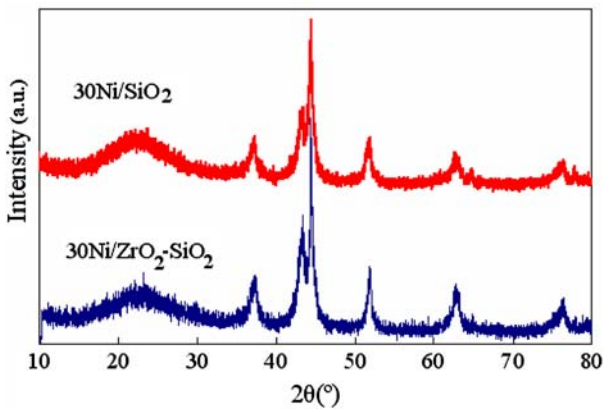

Figure 1. The XRD patterns of $30Ni/SiO_2$ and $30Ni/ZrO_2$–SiO_2 samples.

ZrO_2 content is lower than 30 wt. %, the ZrO_2–SiO_2 composite aerogels are X-ray amorphous due to the incorporation of zirconium atoms in the framework of amorphous SiO_2.

3.1.2. FT-IR analysis

The figure 2 is the FT-IR spectra of $30Ni/SiO_2$, $30Ni/ZrO_2$–SiO_2 and pure SiO_2. For the two catalysts, the peak 964 cm^{-1} assigned to Si-OH bond stretching of SiO_2 [13] decrease indicating a presence of M–O–Si band (in this work M = Zr or Ni) [11,12]. And the $30Ni/ZrO_2$–SiO_2 has the lowest 964 cm^{-1} peak, meaning more M–O–Si bonds are formed.

3.1.3. N_2 adsorption–desorption isotherm analysis

The N_2 adsorption–desorption isotherm analysis results of the two catalysts and the two supports are listed in table 1. Because the supports were not calcined before impregnation, the S_{BET} of the supports are large more than those of the corresponded catalysts. But the addition of ZrO_2 slightly decreases the S_{BET}, and no influence on the isotherm type and pore distribution.

Table 1
The results of N_2 adsorption–desorption isotherm analysis

Samples	S_{BET} (m^2/g)	Pore volume (cm^3/g)
ZrO_2–SiO_2 aerogels support	898	2.14
SiO_2 aerogels support	1015	2.13
$30Ni/ZrO_2$–SiO_2	279	0.38
$30NiO_2/SiO_2$	285	0.39

3.1.4. TPR analysis

The TPR profiles of $30Ni/SiO_2$ and $30Ni/ZrO_2$–SiO_2 are shown on figure 3. The effect of ZrO_2 on the reduction of NiO is clearly shown by the changes of the temperature of the maximum of the main peaks and an upheaval of broad bands at about 500–750 °C.

Comparing the TPR patterns of the sample $30Ni/SiO_2$ and $30Ni/ZrO_2$–SiO_2, we could suppose that the ZrO_2 has an effect of regularity on the interaction strength between the Ni and the ZrO_2–SiO_2 support, that is, decrease the interaction strength of the strong interaction sites and increase the interaction strength of the weak interaction sites, causing the TPR maximum temperature of the main peak slightly move to higher temperature, hunch broad bands at about 500–750 °C and increase hydrogen consumption over the tested temperature range. This regularity effect can be attributed to the higher ionicity of Zr–O bond than that of covalent Si–O band, and the molecular-level mixture of ZrO_2 with SiO_2 matrix.

3.1.5. NH_3-TPD analysis

The NH_3-TPD pattern of the $30Ni/SiO_2$ sample (figure 4. dotted line) is divided into three regions: region I-90–200 °C; region II-200–500 °C and region III-500–800 °C. The $30Ni/ZrO_2$–SiO_2 sample shows a two regions NH_3-TPD pattern (figure 4 solid line): regionI-90–550 °C and region II-550–800 °C. The NH_3-TPD patterns of the supports SiO_2 and ZrO_2–SiO_2

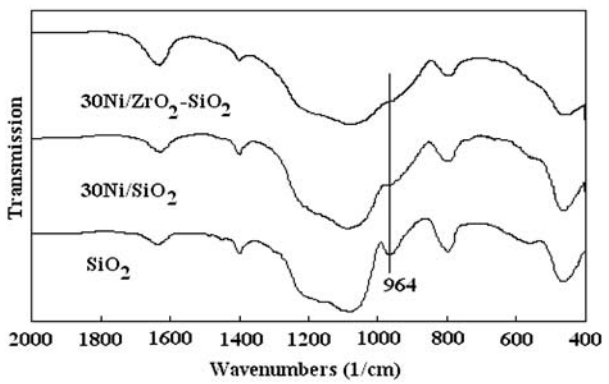

Figure 2. The FT-IR spectra of $30Ni/SiO_2$ and $30Ni/ZrO_2$–SiO_2 samples.

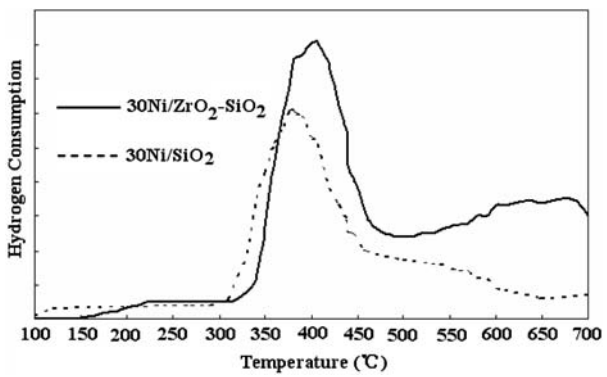

Figure 3. The TPR patterns of $30Ni/SiO_2$ and $30Ni/ZrO_2$–SiO_2 samples.

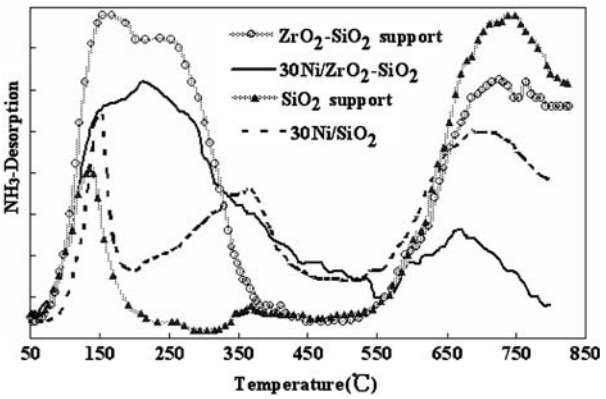

Figure 4. The NH_3-TPD curves of $30Ni/SiO_2$, $30Ni/ZrO_2$–SiO_2, SiO_2 support and ZrO_2–SiO_2 support.

(shown in fig.4 with two transparent labeled lines) are also divided into two regions.

For analysis the factors that affect the acid distribution features, we could roughly treat the 90∼500 °C range as the weak acid region and 500∼800 °C range as the strong acid region. In the weak acid region the acid density is fall in the order of ZrO_2–SiO_2-support, $30Ni/ZrO_2$–SiO_2, $30Ni/SiO_2$ and SiO_2-support. But in the strong acid region, the acid density is fall in the order of SiO_2-support, ZrO_2–SiO_2-support, $30Ni/SiO_2$ and $30Ni/ZrO_2$–SiO_2. Then it could be concluded that the presence of Ni and ZrO_2 both increases the density of weak acid strength sites and decreases the density of strong acid strength sites; but in the strong acid region Ni is the main factor, and in the weak acid region ZrO_2 is the main factor and which is related more with the catalytic selectivity.

The surface acidity of ZrO_2–SiO_2 mixed oxide has been studied intensively by several groups [14–17] and it is widely accepted that the presence of ZrO_2 increase both Lewis and Brønsted acid centers over ZrO_2–SiO_2 mixed oxide.

S. Damyanova and co-workers [14] have studied the acid promotion mechanism of ZrO_2 with x-ray photoelectron spectroscopy (XPS) and FT-IR. They supposed the zirconium is responsible for Lewis acidity in ZrO_2/SiO_2 mixed oxide due to the higher ionicity of the Zr–O bond, and Brønsted acid sites are produced owing to the electron density of the OH bonds is reduced by the Zr–O higher ionicity bonds that are neighboring the more covalent Si–O units.

James A. Anderson and co-workers [15] have especially studied the surface acidity of silica-zirconia aeeogels with different Si/Zr ratio. They also proved the Lewis acid sites originate from zirconia and a roughly linear increase in Lewis acid density as a function of mol% Zr is expectable.

Applying above ideas about the surface acidity generation in ZrO_2–SiO_2 mixed oxides to the $30Ni/SiO_2$ sample, we could believe that the increase of the density of weak acid strength sites is owing to the presence of ZrO_2, and also could suppose most of the increased acid sites are Lewis acid sites. Meanwhile, as the FT-IR and TPR analysis shown (figures 2 and 3), the presence of ZrO_2 also increased the interaction between Ni species and ZrO_2-SiO_2 supports, and more Si–O–M bonds are formed on the surface of $30Ni/ZrO_2$–SiO_2 samples than those formed on the $30Ni/SiO_2$ samples, which decrease the formation of acidic hydroxyls on the surface of the supports and resulting in a decrease of the density of Brønsted acid sites.

3.1.6. Elemental analysis

According to the results of elemental analysis, the Ni content for sample $30Ni/SiO_2$ is 30.15 wt. %; and for sample $30Ni/ZrO_2$–SiO_2, the Ni content is 31.18 wt. %, and the ZrO_2 content is 4.68 wt. %.

3.2. Catalytic test

Table 2 is the results of catalytic hydrogenation of MA. Over the two catalysts, MA was converted com-

Table 2
Catalytic performance of MA hydrogenation on different conditions

Catalyst	Reaction temperature (K)	Reaction pressure (MPa)	Reaction time (h)	MA conversion (%)	GBL selectivity (%)
$30Ni/ZrO_2$–SiO_2	393	6	3	100.0	2.9
	423	6	3	100.0	28.3
	453	6	3	100.0	63.2
	453	3	3	100.0	15.0
	453	4	3	100.0	22.3
	453	5	3	100.0	52.4
	453	6	2	100.0	31.1
	453	6	4	100.0	69.4
	453	6	6	100.0	76.4
	453	6	8	100.0	84.8
$30NiO_2/SiO_2$	453	3	3	100.0	0.7
	453	6	8	100.0	0.6

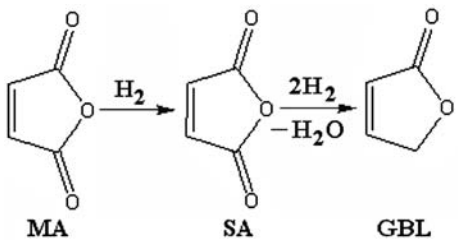

Scheme 1. The catalytic hydrogenation pathway of MA to GBL.

pletely into SA and GBL, and no other relative hydrogenated products were detected. The great difference displayed in the selectivity to GBL. The presence of 5 wt. % ZrO_2 component plays an important role in catalytic selectivity to GBL. On the optimized conditions, over $30Ni/ZrO_2$–SiO_2 the selectivity to GBL is 84.8 %, while over $30Ni/SiO_2$ only small amount of GBL was obtained no matter the reaction conditions.

As shown in Scheme 1, the hydrogenation of MA to GBL follows two-step reactions. Firstly, C=C bond in MA is reduced and converted to SA. And then, GBL is formed via the subsequent oxidative-hydrogenation of C=O bond in SA.

The obvious enhancement of the selectivity to GBL over $30Ni/ZrO_2$–SiO_2 can be explained by the modification of its surface electronic properties towards the improved adsorption of C=O bonds.

Just as the acid promotion mechanism of ZrO_2, firstly, we can attribute the effect of activation of C=O bond to the possible presence of Zr^{4+} species on the catalyst surface owing to the higher ionicity of the Zr–O bonds. And another reason for the increase of the selectivity to GBL could attribute to the proper interaction of Ni with the ZrO_2–SiO_2 support that is regulated by the presence of ZrO_2.

Comparing with other reported liquid-phase MA hydrogenation systems [1–10], the advantage of this $30Ni/ZrO_2$–SiO_2 catalyst is that the GBL can be obtained with a high yield via a one-step continuous operation and no other by-products are formed besides the SA. And it could be proposed that nickel based catalyst supported on ZrO_2–SiO_2 composite aerogels can be an effective one-step catalyst for hydrogenation of MA to GBL.

4. Conclusions

The promotional effects of ZrO_2 on nickel catalyst supported on ZrO_2–SiO_2 composite aerogels were studied systematically. The results indicates that the introduction of ZrO_2 into SiO_2 matrix greatly improved the selectivity to GBL than that on SiO_2 supported Ni catalysts. And it could be proposed that nickel based catalyst supported on ZrO_2–SiO_2 composite aerogels can be an effective one-step catalyst for hydrogenation of MA to GBL.

In the catalysts, the presence of Ni and ZrO_2 both increases the density of weak acid strength sites and decreases the density of strong acid strength sites; but in the strong acid region Ni is the main factor, and in the weak acid region ZrO_2 is the main factor and which is related more with the catalytic selectivity.

The presence of ZrO_2 in the catalyst also has an effect of regularity on the interaction strength between the Ni and the ZrO_2–SiO_2 support.

Acknowledgments

This work is supported by the Industry Development Fund of Shanxi Province (041122 and 031099).

References

[1] U. Herrmann and G. Emig, Ind. Eng. Chem. Res. 371(1998) 759.
[2] U. Herrmann and G. Emig, Ind. Eng. Chem. Res. 36(1997) 2885.
[3] R.M. Deshpande, V.V. Buwa, C.V. Rode, R.V. Chaudhari and P.L. Mills, Catal. Commun 3 (2002) 269.
[4] Y. Hara and K. Takahashib, Catal. Surveys from Jpn 6 (2002) 73.
[5] S.M. Jung, E. Godard, S.Y. Jung, K.-C. Park and J.U. Choi, J. Mol. Catal. A: Chem 198 (2003) 297.
[6] S.M. Jung, E. Godard, S.Y. Jung, K.-C. Park and J.U. Choi, Catal. Today 87 (2003) 171.
[7] J. Xu, K. Sun, L. Zhang, Y. Ren and X. Xu, Catal. Commun 6 (2005) 462.
[8] J. Xu, K. Sun, L. Zhang, Y. Ren and X. Xu, Catal. Lett 107 (2006) 5.
[9] H. Jeong, T.H. Kim, K.I. Kim and S.H. Cho, Fuel Proc. Tech 87 (2006) 497.
[10] T. Hu, H. Yin, R. Zhang, H. Wu, T. Jiang and Y. Wada, Catal. Commun 8 (2007) 193.
[11] Z.-G. Wu, Y.-X. Zhao and D.-S. Liu, Microporous Mesoporous Mater 68 (2004) 127.
[12] Z. Yong-Xiang, Q. Xiao-Qin, H. Xi-Cai, X. Xian-Lun and L. Dian-Sheng, Acta Phys.-Chim. Sin 19 (2003) 450.
[13] S.K. Parida, S. Dash, S. Patel and B.K. Mishra, Adv. in Colloid and Interface Sci 121 (2006) 77.
[14] S. Damyanova, P. Grange and B. Delmon, J. Catal. 168 (1997) 421.
[15] J.A. Anderson, C. Fergusson, I. Rodíguez-Ramos and A. Guerrero-Ruiz, J. Catal 192 (2000) 344.
[16] S. Damyanova, L. Petrov, M.A. Centeno and P. Grange, Appl. Catal. A: General 224 (2002) 271.
[17] C. Flego, L. Carluccio, C. Rizzo and C. Perego, Catal. Commun 2 (2001) 43.